Deep-Sea Research II ▮ (▮▮▮▮) ▮▮▮–▮▮▮

Contents lists available at ScienceDirect

Deep-Sea Research II

journal homepage: www.elsevier.com/locate/dsr2

Thin phytoplankton layer formation at eddies, filaments, and fronts in a coastal upwelling zone

T.M. Shaun Johnston [a,*], Olivia M. Cheriton [b], J. Timothy Pennington [c], Francisco P. Chavez [c]

[a] Scripps Institution of Oceanography, University of California, San Diego, 9500 Gilman Drive, Mail Code 0213, La Jolla, CA 92093, USA
[b] Ocean Sciences Department, University of California, Santa Cruz, 1156 High Street, Santa Cruz, CA 95064, USA
[c] Monterey Bay Aquarium Research Institute, 7700 Sandholdt Road, Moss Landing, CA 95039, USA

ARTICLE INFO

Article history:
Accepted 18 August 2008

Keywords:
Thin layers
Upwelling relaxation
Current shear
Stratification
Transition layer
Monterey Bay

ABSTRACT

On two cruises in August and September 2003 (hereafter cruises 2 and 3) during wind relaxations and transitions to upwelling conditions, thin layers of phytoplankton were observed in or a few meters below the stratified transition layer at the mixed layer base and in regions of sheared flow on the flanks of eddies, filaments, and fronts near Monterey Bay, California. On an earlier cruise in August (cruise 1), no thin layers were found after a prolonged wind relaxation. Chlorophyll concentrations and shear were both an order of magnitude less than on cruises 2 and 3. Our vertical profiles were made using a fluorometer mounted on a conductivity–temperature–depth package, which was lowered from the ship as slowly as 0.25 m s^{-1} every 10 km on five ~80-km cross-shore transects. Remotely sensed sea-surface temperature, chlorophyll, and currents are required to understand the temporal and spatial evolution of the circulation and to interpret the quasi-synoptic *in situ* data. Decorrelation scales are ~20 km from lagged temperature and salinity covariances. Objectively mapped sections of the *in situ* data indicate the waters containing thin layers were recently upwelled at either the Point Sur or Point Año Nuevo upwelling centers. Spatially limited distributions of phytoplankton at the coastal upwelling centers (~40 km alongshore, 20 km cross-shore, and 30 m thick) were transformed into thin layers by current shear and isolated from wind-driven vertical mixing by the stratification maximum of the transition layer. Vertically sheared horizontal currents on the flanks of the eddies, filaments, and fronts horizontally stretched and vertically thinned phytoplankton distributions. These thin, elongated structures were then observed as thin layers of phytoplankton in vertical fluorescence profiles at four stations on cruise 2 and eight stations on cruise 3. Light winds during relaxations did not mix away these thin layers. On cruise 2, thin layers were found at eddies at the inshore and offshore ends of a 100-km-long filament, while broader subsurface chlorophyll maxima were found along the filament. This result suggests that higher-resolution sampling along and across a filament may find thin layers forming and dissipating along its length. On cruise 3, thin layers were found at three adjacent stations across an upwelling front and may have extended continuously for >20 km, but neither species composition nor bio-optical data are available to confirm this conjecture. The thin layers were 1–5 m thick in the vertical at full width half maximum and had peak fluorescence values from 7−30 mg m^{-3}. (Bottle chlorophyll samples showed fluorometer chlorophyll readings may have been 1.3−1.5 × too large, but the scatter in this relation was considerable especially at the larger fluorescence values detected in thin layers.) While sheared currents thinned an initially thick subsurface chlorophyll maximum into thin layers, the peak values in these thin layers exceeded concentrations in the upwelled source waters and were unexplained by our data.

1. Introduction

1.1. Autonomous Ocean Sampling Network II

The Autonomous Ocean Sampling Network II (AOSN II) experiment combined ocean models with observations from autonomous platforms (gliders, autonomous underwater vehicles, drifters, profiling floats), *in situ* instruments (on ships, moorings, and towed bodies), and remote sensors (coastal radar, aircraft, and

* Corresponding author.
E-mail address: shaunj@ucsd.edu (T.M.S. Johnston).

0967-0645/$ - see front matter © 2008 Elsevier Ltd. All rights reserved.
doi:10.1016/j.dsr2.2008.08.006

satellites) to observe and predict the physics and biology of a coastal upwelling zone (Ramp et al., 2008). We contributed broad surveys of currents, hydrography, and chlorophyll-related fluorescence on three cruises (2–6 August, 21–25 August, and 3–6 September 2003) in the Monterey Bay region (Fig. 1). Our ship-based vertical profiles provided a relatively rapid, quasi-synoptic assessment of the subsurface oceanic mesoscale within which spatially limited measurements were made by other slowly moving platforms.

1.2. Observations of thin layers

During cruises 2 and 3, we observed thin layers (<5-m thick in the vertical) of phytoplankton, which are difficult to resolve with typical shipboard measurements and are far below the vertical resolution of regional models. The physical and biological mechanisms forming and maintaining these thin layers in different locations and under different physical conditions is an active area of research. Here, we document thin layers associated with mesoscale flows in a coastal upwelling zone.

Within the last decade, novel optical, acoustical, and water sampling instrumentation have produced centimeter- or meter-scale descriptions of plankton distributions (Cowles et al., 1993; Franks and Jaffe, 2001; Wolk et al., 2002; Holliday et al., 2003; Maar et al., 2003; Lunven et al., 2005; Sutor et al., 2005). Planktonic thin layers may extend horizontally for kilometers and persist for days (Dekshenieks et al., 2001; Rines et al., 2002; Holliday et al., 2003; McManus et al., 2003, 2005; Churnside, 2007). A thin layer is defined operationally as <5 m in vertical extent at full width half maximum, with a peak concentration >3× the ambient background, and reproducible in subsequent profiles (Dekshenieks et al., 2001). However, in the observations presented here, we usually have only single casts at each station. In-layer planktonic densities can be orders of magnitude greater than those just above or below the structure (e.g., Donaghay et al., 1992). Frequently, multiple thin layers occur in a single vertical profile, each with a distinct plankton assemblage (Rines et al., 2002; Lunven et al., 2005). Traditional sampling methods, usually performed with bottles mounted on conductivity–temperature–depth (CTD) profilers may not detect features with vertical spatial scales less than several meters. Careful data interpretation is needed because fluorescence patchiness may also be due to species variability and physiological variability within a single species caused by historical light exposure and nutrient availability (Eisner and Cowles, 2005; Sutor et al., 2005).

The vertical distribution of plankton in layers with large vertical gradients has potentially significant ecological consequences, including increased nutrient fluxes, unique species composition, increased predator/prey encounter, increased export from the upper ocean due to increased aggregation and sinking, and enhanced water column productivity (Cowles et al., 1993; McManus et al., 2003; Ryan et al., 2005; Sutor et al., 2005). Thin phytoplankton layer depth was closely associated with the depth and strength of the pycnocline (Dekshenieks et al., 2001; Rines et al., 2002; Sutor et al., 2005). Thin layers can be composed of taxa whose distribution is restricted to these single layers (Rines et al., 2002) or are present throughout the water column in weaker concentrations (McManus et al., 2003). At present there is an operational distinction between a thin layer and subsurface chlorophyll maximum, but it is uncertain whether the high plankton concentration in a thin layer is a result of successful occupation of an ecological niche or simply a consequence of the physics.

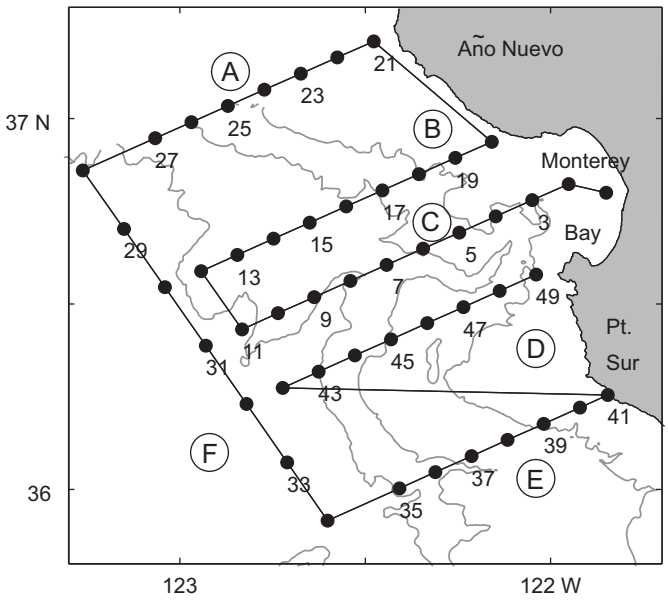

Fig. 1. The cruise track for all three cruises. Cross-shore transects are labeled A–E from north to south and the alongshore transect is F. Transect C is along CalCOFI line 67. Hydrographic stations are numbered in order of occupation and have a spacing of 10 and 20 km on the cross-shore and alongshore transects. Stations 1, 3, and 6 are located near MBARI moorings C1, M1, and M2. Stations 11, 12, and 42 were omitted on cruise 3 in the interest of time. Bathymetry is contoured at 1000, 2000, 3000, and 4000 m.

1.3. Current shear, stratification, and thin layers

The transition layer between the surface mixed layer and the weakly stratified interior is typically a 10–30-m thick, moderately turbulent region defined by maxima below the mixed layer in thermohaline variance, stratification, current shear, and potential vorticity (Johnston and Rudnick, 2008). Mixed-layer depth is a proxy for energy recently input to vertical mixing. Thinner phytoplankton and transition layers were found at the base of shallower mixed layers, where vertical mixing was weaker and stratification was stronger (Dekshenieks et al., 2001; Johnston and Rudnick, 2008). This suggests that the thickness and depth of thin layers are related to the thickness and depth of the transition layer.

The stratification maximum and moderate turbulence in the transition layer can increase phytoplankton concentrations in two ways. Firstly, sinking of large aggregations of phytoplankton may be slowed by changes in stratification at density steps and this convergence may lead to elevated concentrations (Derenbach et al., 1979; MacIntyre et al., 1995). Secondly, moderate turbulence in the transition layer can increase plankton concentrations there by preventing sinking through the pycnocline by mixing aggregations upward (MacIntyre et al., 1995). In a one-dimensional model, sinking organic matter of any type will lead to a deep biomass maximum (Hodges and Rudnick, 2004). The magnitude of the deep biomass maximum depends mostly on sinking rate and diffusivity, while its depth depends mostly on phytoplankton growth rate (Hodges and Rudnick, 2004). These intriguing results further suggest the effects of the stratified and moderately turbulent transition layer on the magnitude of chlorophyll maxima is of first order. However, realistic values of vertical convergence due to different sinking rates in the mixed layer, transition layer, and the interior cannot produce thin layers in the Hodges and Rudnick (2004) model (B. Hodges, personal communications).

Another process contributing to thin layer formation is the vertical shear of horizontal currents (Franks, 1995; Osborn, 1998;

Please cite this article as: Johnston, T.M.S., et al., Thin phytoplankton layer formation at eddies, filaments, and fronts in a coastal upwelling zone. Deep-Sea Research II (2008), doi:10.1016/j.dsr2.2008.08.006

Birch et al., 2008). A thick patch (i.e. a vertically broad distribution of limited lateral extent) of phytoplankton with weak horizontal gradients can be stretched by current shear into vertically thin and horizontally elongated layers, which are then observed as thin layers in vertical profiles. Indeed, any finite patch of tracer will form thin layers due to vertical current shear and such layers in biological and chemical properties should be ubiquitous in the ocean (Birch et al., 2008). However, if stratification is weak, shear instability will cause turbulent mixing and broaden these layers. While biological processes likely contribute to thin layer formation and intensification, thin layers will likely be found in the transition layer, where stratification and current shear are strongest.

Birch et al. (2008) provide a theoretical basis for thin layer formation by current shear and a numerical evaluation in an advection–diffusion model. For example, steady current shear ($s = 10^{-2}\,s^{-1}$) can transform a thick patch with an initial horizontal extent $L_0 = 1\,km$ into a thin layer with minimum thickness $H_{min} \sim (s^{-1}\kappa L_0)^{1/3} = 2\,m$ on a timescale of $t_{min} \sim (s^{-2}\kappa^{-1}L^2)^{1/3} = 12\,h$ assuming a vertical diffusivity of $\kappa = 10^{-4}\,m^2\,s^{-1}$. The initial thickness, H_0, is 10 m, but H_{min} does not depend on H_0. During shear thinning, the thickness changes by an order of magnitude, but the peak intensity decreases by a smaller factor to $I_{min} = 0.6I_0$ at t_{min}, where I_0 is the initial intensity. Also at t_{min}, the thin layer spreads over a horizontal distance of $L_{min} \sim H_0^2\,(3s\kappa^{-1}L_0^2)^{1/3} = 70\,km$. After reaching minimum thickness, vertical diffusion becomes important, the layer broadens, and its intensity decays. The lifetime of the thin layer is estimated as the time from when $H = 2H_{min}$ to the time when $I = 0.5I_{min}$, which is $1.5t_{min}$ or 18 h. Shear acting on a finite nutrient patch (i.e. a coastal upwelling zone) and subsequent phytoplankton growth also produces thin layers of similar thickness, extent, and lifetime. Our observations resolve these spatial and temporal scales.

Also internal waves can strain and shear the water column and have been proposed as a reversible mechanism which produces periodic thin features in a passive tracer (Franks, 1995). For typical near-inertial internal wave shears, 2-m thick layers could be expected to extend horizontally ~1 km (Franks, 1995). Dekshenieks et al. (2001) found a bimodal thin layer distribution with one mode at low shear ($0-0.025\,s^{-1}$) and another at moderate shear ($0.025-0.05\,s^{-1}$). Only 5% of thin layers occurred at shears greater than $0.05\,s^{-1}$. Fluorescence layers were found at a front and a <1-km diameter eddy in Monterey Bay, supporting the idea that thinning occurs via current shear (Ryan et al., 2005).

A general association between mesoscale current shear and finescale phytoplankton layers was found in the coastal upwelling zone off Oregon (Sutor et al., 2005). They surmise that with adequate spatial and temporal resolution, finescale plankton distributions will be found commonly in upwelling areas. Indeed optical measurements from aircraft show thin layers cover 19% of the area surveyed by an 8000-km aircraft survey during wind relaxations in coastal upwelling zones off of California and Oregon (Churnside, 2007). The thin-layer depths were correlated with CTD measurements of vertical density gradients (the variance explained is $r^2 = 0.5$), were 2.2 m thick in the mean, and had a lateral decorrelation scale of 179 m. The observed layers can be continuous for 1–10 km. Given their spatial extent and persistence during relaxations, our ship-based CTD measurements have sufficient spatial and temporal resolution to detect thin layers. Although upwelling brings nutrient-rich water to the surface and increases current shear that transforms thick patches into thin layers, the strong winds rapidly erase thin layers through vertical mixing (Donaghay and Osborn, 1997; Churnside, 2007). However, increased stratification due to fresh water input or lighter winds during wind relaxations promotes thin layer formation (Churnside, 2007).

In this contribution, we infer an initially broad distribution of phytoplankton produced in a coastal upwelling zone was transformed by current shear at eddies, filaments, and fronts into vertically thin and horizontally elongated layers, which were then found in the transition layer as thin layers of phytoplankton in vertical fluorescence profiles.

1.4. Circulation patterns near Monterey Bay

On the central California shelf, coastal upwelling and the California Current system are the main mesoscale and large-scale flow features. In the spring and summer, the coastal upwelling system on the central California shelf switches between two main states: upwelling and relaxation (Rosenfeld et al., 1994). Transitions occur in 1–2 days. During relaxations, southward wind speeds are $<3\,m\,s^{-1}$ or winds are northward (Fig. 2; Roughan et al., 2005). During upwelling, a band of cold water upwells at Año Nuevo and flows southward across the mouth of Monterey Bay (Fig. 1). Another upwelling center is found south of Monterey Bay at Point Sur. Intense submesoscale activity is modeled and observed at upwelling fronts and decays offshore (Capet et al., 2008).

Within Monterey Bay, a cyclonic (counter-clockwise) eddy is found during upwelling. An anticyclonic (clockwise) circulation, typified by warm surface water temperatures, is often observed to the west of the band of cold water flowing across the mouth of Monterey Bay and is a semi-permanent feature, which may be a meander of the California Current (Ramp et al., 2005; Rosenfeld et al., 1994) or California Current jet (Collins et al., 2003). During wind relaxations, these circulation features decay, sometimes reverse, and the anticyclonic eddy translates shoreward.

Spatially and temporally variable upwelling produces cold, saline, and nutrient-rich surface water at the coast, which is transported offshore in squirts, eddies, and meanders (Strub et al., 1991). Topography, such as headlands, can produce local wind relaxations leading to flow convergence and export of coastal waters offshore in narrow filaments, known as squirts. Pairs of counter-rotating eddies produce convergent flow and similar patterns to squirts. The California Current system often meanders onshore, entrains water from the coastal zone, and transports it further offshore.

2. Methods

2.1. Data

On three cruises on R/V *Point Sur* from 2–6 August, 21–25 August, and 3–6 September 2003 (hereafter cruises 1, 2, and 3),

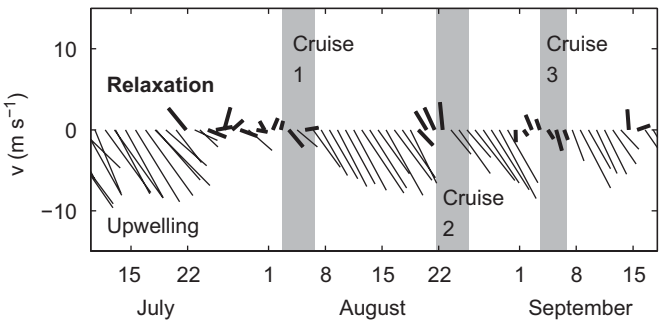

Fig. 2. Daily mean wind vectors measured at the MBARI M2 mooring near station 6 from July to September 2003. The three cruises are indicated by gray shading. Upwelling-favorable winds are southward. Vectors show the direction towards which the wind is blowing (north is up, east is right). Relaxation from upwelling conditions is defined as southward winds with speeds $<3\,m\,s^{-1}$ or northward winds. Relaxed winds are denoted by bold vectors.

Please cite this article as: Johnston, T.M.S., et al., Thin phytoplankton layer formation at eddies, filaments, and fronts in a coastal upwelling zone. Deep-Sea Research II (2008), doi:10.1016/j.dsr2.2008.08.006

five cross-shore transects (~80-km long, oriented 61° to true north) and one alongshore, 100-km long transect were completed in Monterey Bay and adjacent waters (Fig. 1). Along these transects, 49 hydrographic stations were occupied at a spacing of 10 km nearshore and 20 km offshore. On cruise 3, three stations were omitted due to time constraints.

Two rosettes were each equipped with a Sea-Bird 911+ CTD measuring conductivity, temperature, and pressure; a WET Labs C-Star transmissometer measuring beam attenuation at 660 nm wavelength; and a WET Labs ECO-FL fluorometer to provide chlorophyll *a* fluorescence as an indicator of chlorophyll or phytoplankton concentration. The fluorometer had a sampling rate of 8 Hz, while the CTD sampled at 24 Hz. The intakes for the fluorometer and the CTD were on the bottom of each rosette with intakes on the same level. From these measurements, depth (z) and profiles of salinity (S), temperature (T), and potential density (σ_θ) were calculated from downcasts at a vertical resolution of 0.3 m, which was possible due to exceptionally calm seas and descent rates as low as 0.25 m s^{-1}. Ship roll was small enough that typically >8 samples of CTD data were averaged into each 0.3-m bin.

A standard fluorometer calibration from WET Labs was used to obtain chlorophyll. Fluorometer chlorophyll readings on upcasts were 1.3−1.5× bottle chlorophyll from a linear regression against bottle chlorophyll (in the range of 0–2 or 0−4 mg m^{-3} depending on the cruise and CTD package used). There was considerable scatter in this relation (the variance fraction explained by a linear regression: $r^2 = 0.33-0.83$) especially at high fluorescence values perhaps due to the uncertainty in the exact depth at which bottles were triggered and difficulty sampling thin layers with bottles. Fluorometer data were not adjusted because: (1) there were few comparisons between bottle data and high fluorescence values at thin layers, (2) scatter at high chlorophyll values was considerable, and (3) the value of the fluorescence peak would have been affected, but any adjustment would not have affected layer thicknesses or conclusions made in this paper. The peak fluorescence values found in the thin layers are much larger than found in ordinary subsurface chlorophyll maxima despite the scatter at high values. Data presented hereafter are from downcasts with the exception of bottle chlorophyll samples which are from upcasts. Niskin bottles were triggered on the upcasts at 0, 5, 10, 20, 30, 40, 60, 80, and 100 m. These samples were assayed for chlorophyll *a* (Pennington and Chavez, 2000).

Thin layers were identified in upcasts and downcasts. Sometimes the passage of the rosette mixed the water on the downcast making the fluorescence maximum thicker on the upcast than the downcast (Lunven et al., 2005). While we did not usually perform multiple casts at a single station, either broader maxima or thin layers on upcasts provided confidence in the detection of thin layers on downcasts. We emphasize that 3–16 data points define these thin layers at full width half maximum. Thus we cannot define persistence based on multiple casts at one location, but we gain further confidence in these measurements by multiple observations of thin layers at the flanks of mesoscale features. Transmissometer data also support the fluorescence data.

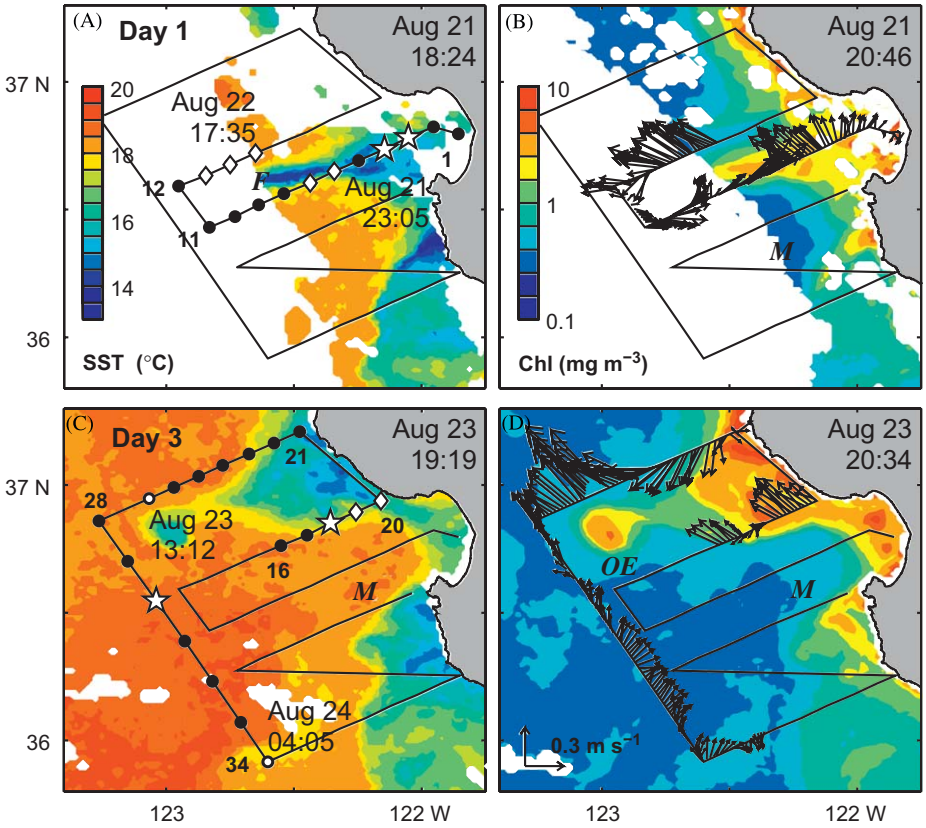

Fig. 3. Sea-surface temperature from AVHRR (left column) and chlorophyll from SeaWIFS (right column) from cruise 2 on days 1 and 3 (top and bottom rows; dates and times in the upper right corners) showed the formation of a cold, chlorophyll-rich filament. The ship track is shown as a solid black line and stations occupied during the time interval between images are shown as black dots with some dates and UTC times annotated in the left column. Note the 1-day gap. ADCP currents at $z = 19$ m are plotted (right). The anticyclonic meander (*M*), filament (*F*), and offshore eddy (*OE*) are labeled (Section 3.3). Thin layers are found at stations denoted with stars, while nearby broader subsurface chlorophyll maxima are denoted with diamonds.

Please cite this article as: Johnston, T.M.S., et al., Thin phytoplankton layer formation at eddies, filaments, and fronts in a coastal upwelling zone. Deep-Sea Research II (2008), doi:10.1016/j.dsr2.2008.08.006

Over the entire survey, eastward and northward currents were obtained with a 150 kHz RD Instruments shipboard acoustic Doppler current profiler (ADCP) from $z = 19-467$ m. Unfortunately, the middle of the first bin was at 19 m and the 8-m depth bins were too coarse for observing finescale shear around thin layers. Therefore, we calculated geostrophic current shear from horizontal density gradients via the thermal wind balance:

$$\partial_z v_r = -g\partial_x \sigma_\theta/(f\rho), \quad (1)$$

where (x, y) are the horizontal coordinates parallel and perpendicular to the cross-shore transects (a rotation of 61° from north with positive to the northeast and northwest, roughly), v_r is the alongshore current, ρ is the *in situ* density, g is the gravitational acceleration, and f is the Coriolis frequency (Gill, 1982). The Monterey Bay area is a generation site of strong internal tides (Petruncio et al., 1998; Kunze et al., 2002; Jachec et al., 2006; Wang et al., 2008) and near-inertial internal waves are always present. Their temporal and spatial variability were likely the main contaminants in our calculations of density and geostrophic current shear. We measured neither the ageostrophic shear nor any alongshore density gradients (i.e. cross-shore shear). Therefore, shears presented here are underestimates.

Sea-surface temperature (SST) from the Advanced Very High Resolution Radiometer (AVHRR) and chlorophyll from the Sea-viewing Wide Field-of-view Sensor (SeaWIFS) were used to provide synoptic images. The satellite data were critical to interpreting our ship-based measurements because the SST and surface chlorophyll patterns translated by >20 km in 24 h and their structures evolved. Additional high resolution surface current data near Monterey Bay were obtained from high-frequency coastal radar (Paduan and Lipphardt, 2003). Daily means of surface currents were calculated from hourly data. Daily mean wind data were calculated from the Monterey Bay Aquarium Research Institute's (MBARI) M2 mooring located near station 6. All dates and times are Coordinated Universal Time (UTC).

2.2. Objective mapping

From laterally sparse CTD casts, we produced vertical objective maps of the data along each transect and horizontal maps at 0.3-m depth intervals. With a known data spatial covariance and signal-to-noise ratio, objective mapping reduces sampling noise, preserves spatial resolution, and provides a mapping error (Le Traon, 1990; Lavender, 2001). The error depends on the sampling

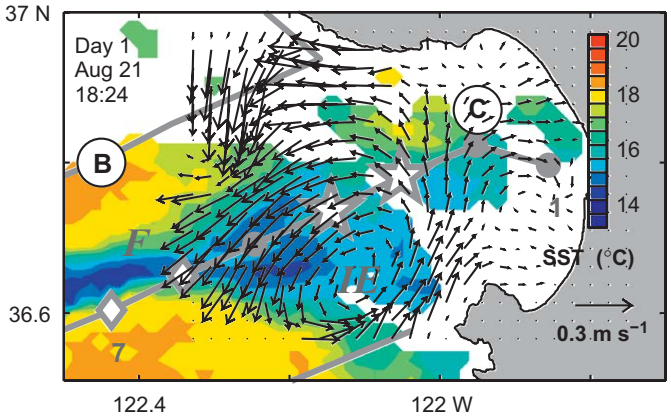

Fig. 4. The CODAR daily mean surface currents are superimposed on sea-surface temperature from AVHRR at 18:24 UTC on 21 August 2003. Gray lines show transects B–D and gray dots indicate stations 1–7, which were occupied within several hours of the SST image. The filament (*F*) and inshore eddy (*IE*) are labeled (Section 3.3). Thin layers are found at stations denoted with stars, while nearby broader subsurface chlorophyll maxima are denoted with diamonds.

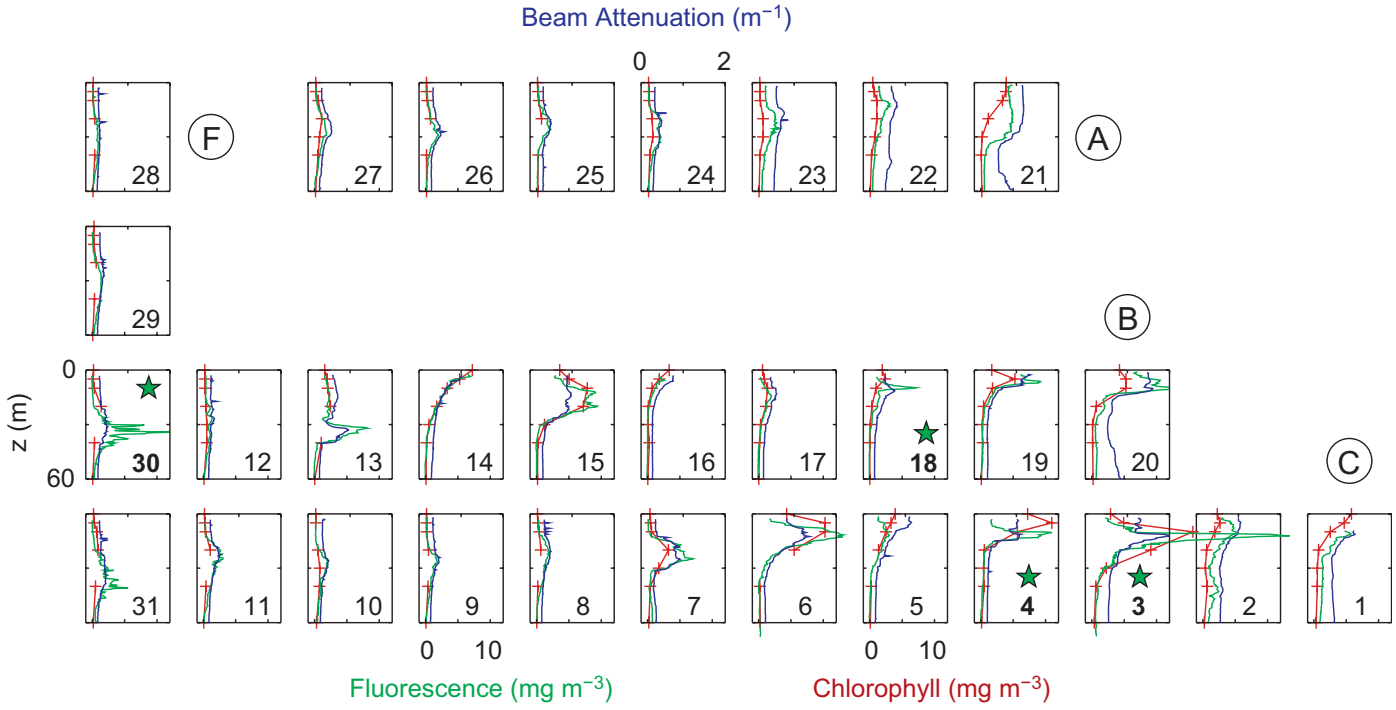

Fig. 5. Vertical profiles of fluorescence (green), chlorophyll *a* from the bottle samples (red), and beam attenuation from the transmissometer (blue) are shown in an approximate geographic layout of transects A–C and F for cruise 2. For all plots, the vertical and horizontal axes are the same with the top axes for attenuation and bottom axes for chlorophyll and fluorescence. Stations with thin layers are denoted by a green star and a bold station number.

Please cite this article as: Johnston, T.M.S., et al., Thin phytoplankton layer formation at eddies, filaments, and fronts in a coastal upwelling zone. Deep-Sea Research II (2008), doi:10.1016/j.dsr2.2008.08.006

grid, data covariance, and signal-to-noise ratio, but not the discrete data values themselves. For example, during cruise 2, we were concerned with a filament (*F* in Fig. 3) sampled by transects B and C. While the region in the vicinity of transects B and C was sampled relatively well with objectively mapped errors of <0.2 of the covariance, the regions between transects A and B displayed a much larger error of >0.7 of the covariance.

Rather than performing computationally costly calculations to make a fully three-dimensional map, we made two sets of two-dimensional maps: vertical planes along the cross-shore transects and horizontal planes at constant depth. Horizontal maps were constructed for T, S, σ_θ, and fluorescence at 0.3-m intervals from 0 to 100 m from which data are interpolated onto isopycnal surfaces. For horizontal and vertical sections, we used different decorrelation scales of 20 and 10 km in the horizontal and noise levels of 5% and 0.5% of the data–data covariance. A 20-km scale was used for the horizontal sections allowing stations on adjacent transects to influence results. The weighting on vertical sections was limited to adjacent stations on the same transect. The vertical sections had a vertical decorrelation scale of 10 m. The decorrelation scales used here were not large enough to smooth over unresolved processes, such as internal waves and internal tides. The noise levels were assumed to be small for the vertical sections because we do not want to permit excessive smoothing of the data and noise levels are larger for the horizontal sections because of the time needed to sample the larger area.

These sections were quasi-synoptic, as the satellite data will show. While our station resolution was too coarse to replicate the sharp features observed by satellite, the *in situ* sampling revealed intriguing subsurface structures and broadly captured the horizontal spatial structure. We took more than 16 h to complete the middle transect and four days for the whole survey. A typical decorrelation scale for the coastal ocean can be estimated as the diameter of an eddy originating from baroclinic instability, which is $\pi L_R > 50$ km in the deeper waters of our survey region, where the internal Rossby radius of deformation (L_R) is >15 km (Rosenfeld et al., 1994). This eddy diameter is similar to observed decorrelation scales further south on the California coast of 58 km in the alongshore direction during wind relaxations (Dever, 2004). However, a 20-km cross-shore scale is obtained from lagged correlation of our T–S data in agreement with decorrelation e-folding scales of 1.5 days and 15 km calculated from gliders during AOSN II (Davis et al., 2008). Other more reactive tracers such as phytoplankton may have smaller decorrelation scales (Mahadevan and Campbell, 2002), but given the resolution of our sampling array we use a single scale for all variables. Adjacent transects (except for transects C and D, which were sampled three days apart) were roughly synoptic, while our entire four-day survey pattern sampled flow features evolving in space and time.

3. Results from cruise 2 (21–25 August 2003)

3.1. Overview

Thin layers were found on the flanks of three mesoscale features of recently upwelled water: a filament of cold, chlorophyll-rich coastal water extending offshore from Monterey Bay (*F* in Figs. 3A, B and 4); an offshore eddy (*OE*) at the tip of the filament (*OE* in Figs. 3C, D); and an inshore eddy (*IE*) at the base of the filament in Monterey Bay (*IE* in Fig. 4). In the following subsections, we describe the mesoscale circulation, the characteristics of the thin layers, and how the thin layers are formed on the flanks of mesoscale flows.

3.2. Mesoscale patterns

First, we describe mesoscale circulation, SST, and sea-surface chlorophyll patterns. After upwelling-favorable (southward) winds from 7 to 19 August 2003, the winds relaxed two days prior to the cruise and for cruise days 1–3 with wind speeds

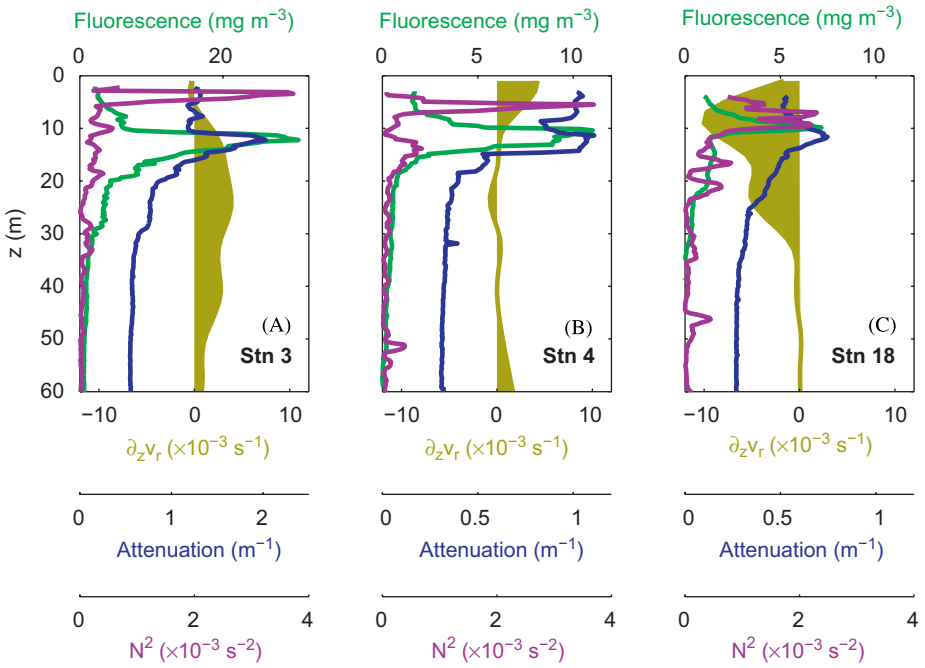

Fig. 6. Individual profiles from cruise 2 of fluorescence (green), alongshore geostrophic current shear from thermal wind (brown shading is used to distinguish positive and negative shear), beam attenuation (blue), and buoyancy frequency (purple) from some of the stations which showed thin layers: (A) station 3, (B) station 4, and (C) station 18. A five point running mean filter with a total length of 1.5 m is applied to smooth the buoyancy frequency. Note the scales for fluorescence and beam attenuation in (A) are different from (B) and (C).

Please cite this article as: Johnston, T.M.S., et al., Thin phytoplankton layer formation at eddies, filaments, and fronts in a coastal upwelling zone. Deep-Sea Research II (2008), doi:10.1016/j.dsr2.2008.08.006

$<3\,m\,s^{-1}$ (Fig. 2, 19–23 August 2003). Upwelling-favorable winds resumed on cruise day 4 (24 August 2003). At the surface near the coastal upwelling centers of Points Año Nuevo and Sur, the upwelled water was cool ($T\sim12-15.5\,^{\circ}C$, Fig. 3) and salty ($S\sim33.5$ psu). Phytoplankton concentrations were also high ($\sim5\,mg\,m^{-3}$, Figs. 3 and 5). Surface waters away from the upwelling centers were mostly warmer ($T\sim20\,^{\circ}C$), fresher ($S\sim33$ psu), and phytoplankton concentrations were lower ($<1\,mg\,m^{-3}$).

One day prior to cruise 2, cold and chlorophyll-rich water was found at the upwelling center at Point Sur. By cruise day 1, the anticyclonic meander of warm, chlorophyll-poor, offshore water reached the coast between Point Sur and Monterey Bay separating the upwelling at Point Sur from the narrow filament of cold, chlorophyll-rich water (Figs. 3C, D, 21 August 2003). The middle transect C crossed the filament (*F* at stations 5–6, Fig. 3). A current jet was observed with CODAR at the filament (*F* in Fig. 4). By cruise day 3, the meander and filament had translated further northward. Near Point Año Nuevo between the two northernmost transects, currents converged at the base of the filament near the coast and another anticyclonic meander of warm, chlorophyll-poor offshore water was found just to the north of the survey (Figs. 3C, D).

During upwelling conditions, cyclonic circulation is found within Monterey Bay and the *IE* was located within the bay prior to cruise 2. Under relaxed winds, the *IE* moved ~20 km offshore by one day prior to the cruise and was replaced by an anticyclonic eddy on cruise day 1 (Fig. 4 on 21 August 2003). The middle transect crossed the flanks of the filament and inshore cyclonic eddy (*F* and *IE* at stations 3–7 in Fig. 4).

The cyclonic eddy at the offshore tip of the filament was located between transects B and C and showed up clearly in the ADCP currents (Fig. 3B). On cruise day 2, transect B intersected the cyclonic *OE* at the tip of the filament at (stations 13–15, Fig. 3B on 22 August 2003). Between cruise days 2 and 3, the *OE* at the filament's tip passed near the offshore transect (stations 30–31, Figs. 3C, D on 22–23 August 2003).

3.3. Locations and characteristics of thin layers

Thin layers were found on the flanks of the *IE* (stations 3–4), filament (*F*, station 18), and the *OE* (station 30, thin layers denoted by stars in Figs. 3–5). The *IE* was located at the base of the filament, while the *OE* was found at the tip of the filament (Figs. 3 and 4). Broader fluorescence features with vertical thicknesses >5 m at full width half maximum were observed adjacent to the thin layers near the *IE* (stations 1, 2, 6, 7; Fig. 4), filament (*F*, stations 19–20, Fig. 3), and the *OE* (stations 13–15, and 31; Fig. 3).

Bottle samples taken on upcasts were analyzed for chlorophyll and showed subsurface maxima at these stations, but the vertical

Table 1
Subsurface fluorescence peaks are described at the filament and eddies for cruise 2, where z_{max} is its depth, F_{max} is its peak value, z_{fwhm} is its full width at half maximum, and σ_θ is the potential density at z_{max}

Stn.	z_{max} (m)	F_{max} (mg m^{-3})	z_{fwhm} (m)	σ_θ (kg m^{-3})	Thin layer
1	11.0	5.7	8.0	25.35	
2	10.4	5.2	17.3	25.23	
3	12.2	30.6	3.3	25.41	Yes
4	10.4	11.0	3.6	25.45	Yes
5	11.9	3.0	16.7	25.59	
6	11.6	13.1	9.8	25.31	
7	24.7	7.0	13.7	25.08	
13	32.2	8.2	7.1	25.57	
14	3.6	7.0	8.3	25.04	
15	20.0	9.4	15.8	25.54	
18	9.8	7.2	1.8	24.91	Yes
19	6.6	9.3	6.0	25.19	
20	10.1	13.5	11.0	25.41	
30	34.2	14.5	4.8	25.14	Yes
31	40.8	5.5	10.4	25.32	

Stn. is the station number and if a subsurface maximum is a thin layer, it is noted.

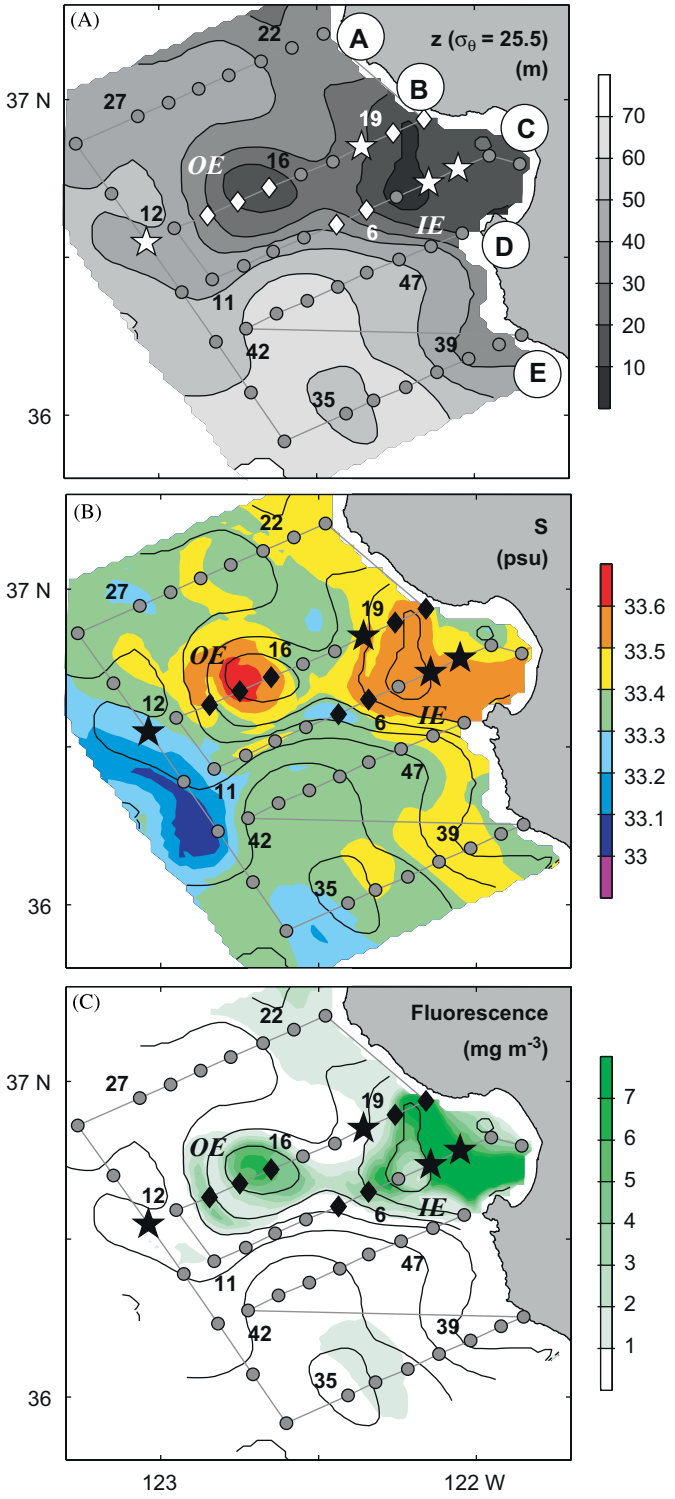

Fig. 7. a) Depths of the $\sigma_\theta = 25.5\,kg\,m^{-3}$ isopycnal for cruise 2 are plotted here and contoured below (black). b) Salinity and c) fluorescence are plotted on $\sigma_\theta = 25.5\,kg\,m^{-3}$. Gray dots indicate CTD stations, stars indicate thin layer locations, and diamonds indicate nearby subsurface chlorophyll maxima. The inshore eddy (*IE*) and offshore eddy (*OE*) are labeled (Section 3.3).

Please cite this article as: Johnston, T.M.S., et al., Thin phytoplankton layer formation at eddies, filaments, and fronts in a coastal upwelling zone. Deep-Sea Research II (2008), doi:10.1016/j.dsr2.2008.08.006

resolution of the bottles did not resolve thin layers seen on downcasts (Fig. 5). Beam attenuation was high at the thin layers and decreased above them indicating the thin layers are subsurface particle maxima (Figs. 5 and 6). Along with upcasts at the same stations with similar profiles (Section 2.1), the transmissometer measurements give us further confidence in the fluorometer measurements of thin layers. The subsurface fluorescence maxima were due to neither photoinhibition near the surface nor spurious fluorometer readings. Near the *IE* and filament, the thin layers at stations 3, 4 and 18 had vertical thicknesses of 1.8–3.6 m at full width half maximum, peak fluorescence values of $7.2-30.6\,\mathrm{mg\,m^{-3}}$, were in the upper 12 m of the water column, and were bounded by $\sigma_\theta = 24.91-25.45\,\mathrm{kg\,m^{-3}}$ (Table 1). The thin layer near the *OE* at station 30 was thicker (4.8 m at full width half maximum), deeper ($z = 34.2$ m), and on $\sigma_\theta = 25.1\,\mathrm{kg\,m^{-3}}$ and had a peak fluorescence value of $14.5\,\mathrm{mg\,m^{-3}}$ (Table 1).

The stratified transition layer is found below the mixed layer and is identified as a peak in the stratification or buoyancy frequency: $N^2 = -g\partial_z\sigma_\theta/\sigma_{\theta_o}$, where g is the acceleration due to gravity and σ_{θ_o} is a reference potential density. The thin layers are found <5 m below the stratification peak (Fig. 6) and are associated with elevated shear at station 18. At stations 3 and 4, the cross-shore shear component in the filament cannot be calculated by geostrophy from our section as noted in Section 2.1, but shear is likely considerable in the strong current jet (Fig. 4).

3.4. Thin layers, shear, and stratification

While the satellite data provided a synoptic picture, our *in situ* sampling broadly captured the recently upwelled, salty water of the *OE*, *IE*, and the filament as shallow depths of an isopycnal ($\sigma_\theta = 25.5\,\mathrm{kg\,m^{-3}}$, Figs. 7A, B). Due to the station spacing, it is difficult to definitively distinguish the filament from either the *OE* or *IE* in the *in situ* data. The thin layers were found within 12 m of the surface at the filament and *IE* and within 34 m of the surface at the *OE*, which suggests the thin layers were subducted as they were advected offshore by the filament (Figs. 7A, C). Most of the thin layers and nearby broader subsurface chlorophyll maxima were associated with a recently upwelled water mass with $S \geqslant 33.5$ psu (Fig. 7B). The thin layer at station 30 had a lower salinity, but was located at a similar depth to the broad chlorophyll maxima in the *OE* (stations 13–15, Fig. 5, Table 1).

A vertical section shows high fluorescence at the flanks of the *IE* or filament (*IE* or *F*, stations 3–4 and 6–7, Fig. 8C), *OE* (stations 13–15, Fig. 8B), and filament (*F*, stations 18–20, Fig. 8B); in or just below the stratified transition layer (Figs. 8H, I); and where vertical shear of horizontal currents is higher (Figs. 8E, F) or expected to be higher in the filament's current jet (*F*, stations 3–4, Fig. 4). The calculated component of shear perpendicular to the middle transect at stations 3 and 4 was low (Figs. 8E, F) because the currents in the filament were aligned almost parallel to the transect (Fig. 4). Along the axis of the filament at station 5, no subsurface chlorophyll maximum is found because the isopycnal outcrops and exposes the water to wind-driven mixing. Shear along the northern transect A was similar and isopycnals sloped upward, but fluorescence values were low in this offshore water (Figs. 7B and 8A).

4. Results from cruise 3 (3–6 September 2003)

4.1. Overview

From 3 to 6 September 2003, cruise 3 found thin layers associated with mesoscale flow: the subducting offshore front of an upwelling tongue (*UT*), an anticyclonic eddy (*AE*) in Monterey Bay, another offshore eddy (*OE*) and another filament (*F*, Fig. 9). In the following subsections, we describe the mesoscale circulation, the characteristics of the thin layers, and how the thin layers are formed on the flanks of mesoscale flows.

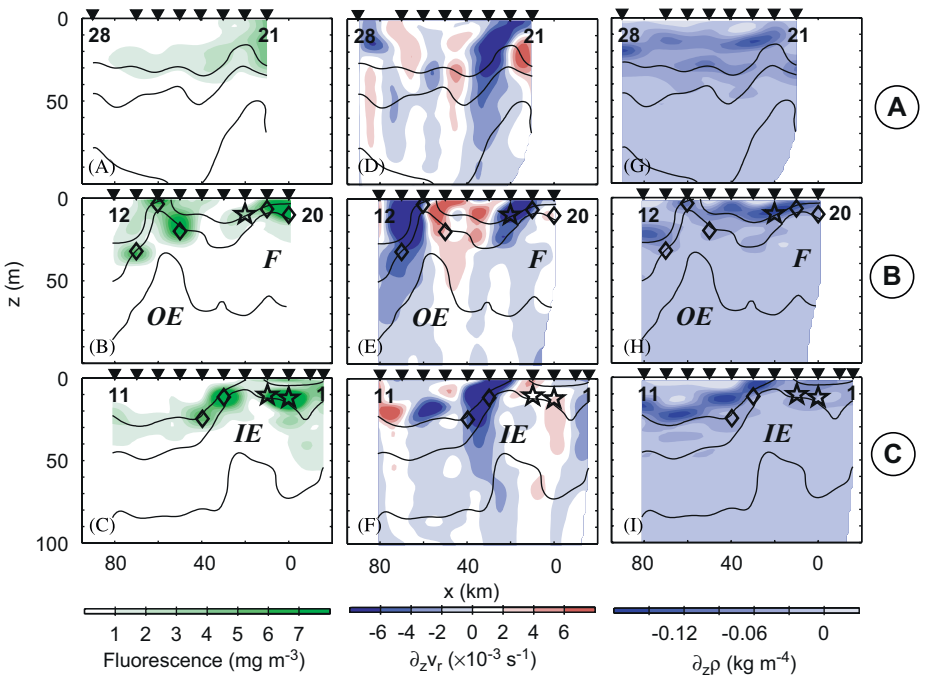

Fig. 8. For cruise 2, cross-shore transects A–C (from north to south; top to bottom of page) of fluorescence (left column, a–c), alongshore geostrophic current shear from the thermal wind equation (middle column, d–f), and vertical density gradient (right column, g–i). x is the cross-shore distance from station 3 on transect C. Contours are $\sigma_\theta = 25.0$, 25.5, and $26.0\,\mathrm{kg\,m^{-3}}$. Black triangles indicate CTD stations. Station numbers are noted at the east and west ends of the transects. The filament (*F*), inshore eddy (*IE*), and offshore eddy (*OE*) are labeled (Section 3.3). Thin layers are indicated with stars and nearby subsurface chlorophyll maxima are denoted with diamonds.

Please cite this article as: Johnston, T.M.S., et al., Thin phytoplankton layer formation at eddies, filaments, and fronts in a coastal upwelling zone. Deep-Sea Research II (2008), doi:10.1016/j.dsr2.2008.08.006

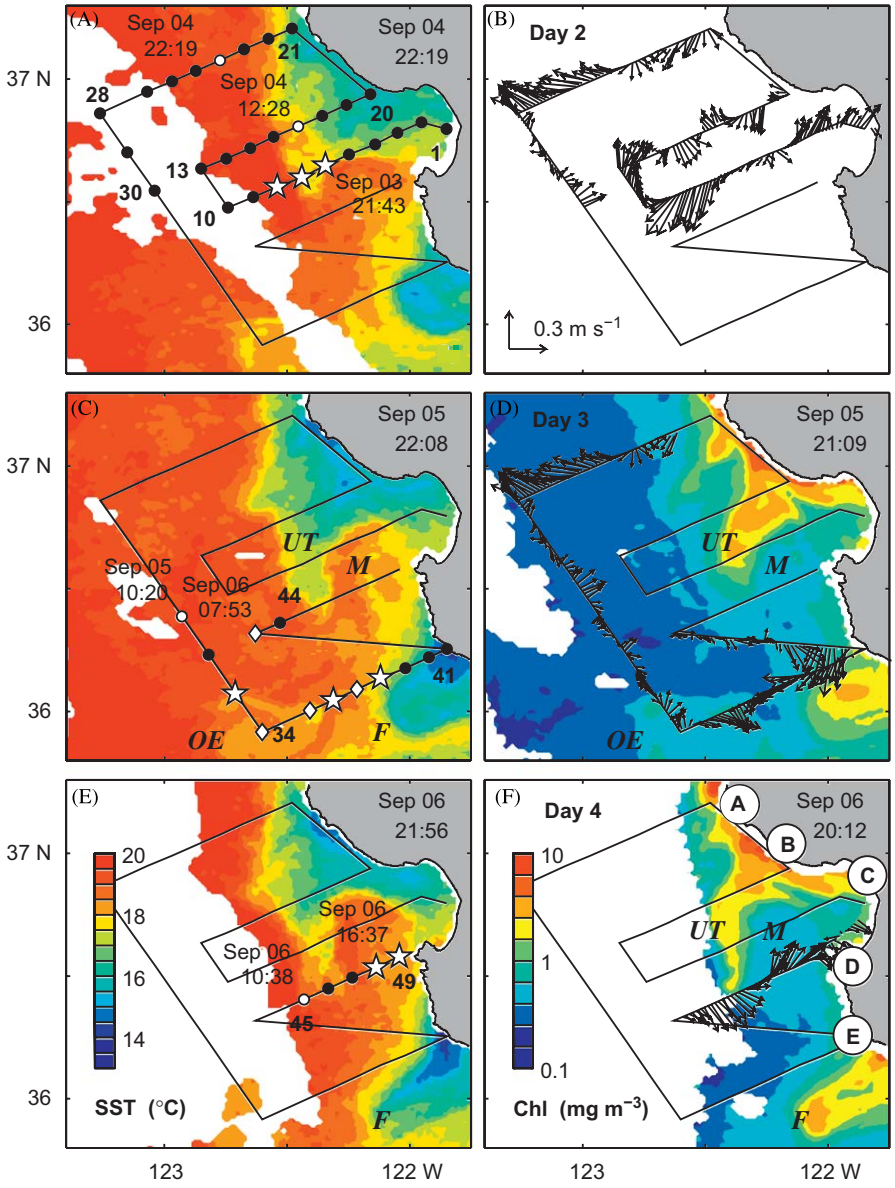

Fig. 9. As for Fig. 3, but for cruise 3. The upwelling tongue (*UT*), meander (*M*), filament (*F*), and offshore eddy (*OE*) are labeled (Section 4.3).

4.2. Mesoscale patterns

First, we describe mesoscale circulation, SST, and sea-surface chlorophyll patterns. The *UT* of cold, chlorophyll-rich water extended southward from Point Año Nuevo reaching stations 6–8 on the middle transect C (Fig. 9A). The *OE* was found at the southwest corner of the survey pattern (first sampled at stations 33–36 and later at station 43, Fig. 9C). The filament's initial growth was observed along the southern transect E (stations 37–41, Fig. 9C). The *AE* near the mouth of Monterey Bay is seen most clearly in the CODAR surface currents (stations 48–49, Fig. 10B).

Between cruises 2 and 3, there were 13 days of upwelling-favorable winds followed by two days of relaxation. Cruise 3 captured the transition from relaxation to upwelling. Initially winds were northward and then $<3\,m\,s^{-1}$ southward (Fig. 2). Upwelling resumed on the day after the cruise (7 September 2003). Recently upwelled waters at Points Año Nuevo and Sur had surface $T\sim12-16\,^{\circ}C$ (Fig. 9), $S\sim33.5$ psu, and chlorophyll in the range of $1-10\,mg\,m^{-3}$ (Fig. 9). Surface waters away from the upwelling centers were mostly warmer ($T\sim20\,^{\circ}C$) and fresher ($S\sim33$ psu) with lower phytoplankton concentrations ($<1\,mg\,m^{-3}$) similar to cruise 2.

4.3. Locations and characteristics of thin layers

Thin layers were observed at the offshore front of the *UT* (stations 6–8), the flanks of the *OE* (stations 33 and 36), the flank of the developing filament (*F*, station 38), and at the *AE* (stations 48 and 49) inshore of an anticyclonic meander (*M*, Fig. 11 and Table 1). Broader subsurface chlorophyll maxima were found adjacent to the *OE* (stations 34, 35, and 43) and the filament (station 37, Fig. 11 and Table 2). In the thin layers, peak fluorescence values were $6.8-16.7\,mg\,m^{-3}$. They had thicknesses from 0.9 to 4.8 m at full width half maximum and were found at depths from 13.4 to 36.9 m and σ_θ from 24.48 to $25.06\,kg\,m^{-3}$. Again there was general agreement of the fluorometer with the transmissometer measurements and water samples (Figs. 11 and 12). Unfortunately, on cruise 3 some of the bottles on the rosette

Please cite this article as: Johnston, T.M.S., et al., Thin phytoplankton layer formation at eddies, filaments, and fronts in a coastal upwelling zone. Deep-Sea Research II (2008), doi:10.1016/j.dsr2.2008.08.006

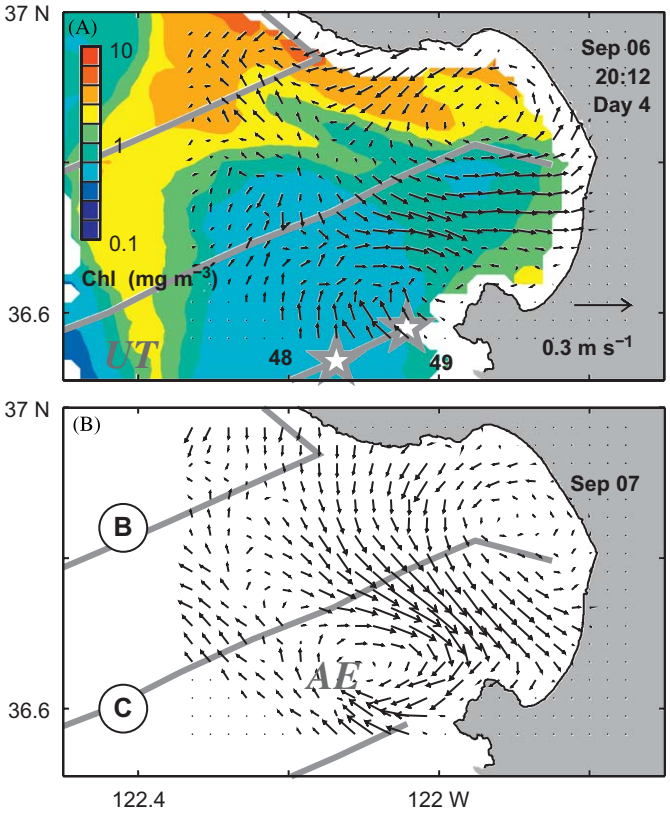

Fig. 10. The CODAR daily mean surface currents from (A) cruise day 4 and (B) one day after the cruise (7 September 2003) are superimposed on sea-surface chlorophyll from SeaWIFS. The upwelling tongue (*UT*) is labeled (Section 4.3). Dates and times are UTC. Gray lines show transects B–D and gray stars in (A) indicate thin layers were found on the flanks of the developing anticyclonic eddy (*AE*) at stations 48 and 49 on cruise day 4.

did not close properly and several data points at the subsurface maxima were missing. Thin layers were found either 5–10 m beneath the stratification maxima or at smaller density steps within the transition layer (Fig. 12). At stations 6, 36, and 38, geostrophic current shear (Figs. 12E, F) likely underestimated the total shear in the *UT*, *OE*, and filament, where currents were nearly parallel to the transect (Figs. 9B, D). Otherwise, geostrophic shear is appreciable near the thin layers in Figs. 12A–D.

4.4. Thin layers, shear, and stratification

The UT: On cruise day 1, the *UT* extended from its origin at the coast north of Monterey Bay southward past the middle transect. The origin of the thin phytoplankton layers in the *UT* (stations 6–8, Fig. 9A) was a broad chlorophyll maximum found at the coast (stations 19–20, Figs. 9D and 11). Cyclonic flow was found in the tongue of cool upwelled water (Figs. 9A, B). By cruise day 3, the *UT* had moved further southward, while the meander had moved further northward (Fig. 9C, 5 September 2003). The *UT* was identified by the shallow depth of the $\sigma_\theta = 24.8\,\mathrm{kg\,m^{-3}}$ isopycnal and higher salinities (Figs. 13A, B). Thin layers were found on the flanks of the *UT* (stations 6–8, Figs. 13C and 14A), several meters below the region of highest geostrophic shear in the front between the *UT* and offshore water (stations 7–8, Fig. 14D), and in the stratified transition layer (stations 6–8, Fig. 14G). We believe vertical shear at the thin layer at station 6 was low (Fig. 14D) because currents were oriented parallel to the transect (Fig. 9B).

The Meander: On cruise day 1, there were no satellite data available, but the image from cruise day 2 showed a northward- and shoreward-migrating, anticyclonic meander of warm, chlorophyll-poor, offshore water just south of the central transect (*M*, Fig. 9A, 4 September 2003). The meander on the inshore side of the *UT* was characterized by the deeper depth of the $\sigma_\theta = 24.8\,\mathrm{kg\,m^{-3}}$ isopycnal and low salinities (Figs. 13A, B).

The AE: Surface currents from CODAR in Monterey Bay showed a transition from relaxation to upwelling: on cruise day 2 a cyclonic eddy was located entirely within the bay (figure on 4 September 2003 not shown), it weakened and migrated westward by cruise day 3 (figure on 5 September not shown), and weakened further by cruise day 4 (Fig. 10A, 6 September 2003). One day after the cruise, upwelling conditions were developed with the *AE* at the mouth of the bay and a cyclonic eddy in the bay (Fig. 10B, 7 September 2003). The thin layers were found at the shear maximum on the inshore flank of the meander or at the *AE* (stations 48–49, Figs. 14B and E) and in the stratified transition layer (Fig. 14H).

The OE: On cruise day 3, the *OE* was also seen in temperature and currents (stations 33–35, Figs. 9C, D). The eddy displayed weak stratification (Fig. 14I), lower temperatures (Fig. 9C), and higher salinities (Fig. 13B) typical of upwelled water. The weak stratification and anticyclonic ADCP-measured currents (Fig. 9D) are typical of intrathermocline eddies (Thomas, 2008). The highly variable vertical fluorescence profile suggests thin layers were actively forming (stations 33–36, Fig. 11) due to the shear in the intrathermocline eddy (a strong geostrophic shear component is found in Fig. 14F). Thin layers were found on the *OE*'s flanks (stations 33 and 36, Figs. 13B, C). On cruise day 4, the *OE*'s flank was sampled again, where a broader subsurface fluorescence maximum was found (station 43, Table 2, satellite image from 8 September 2003 not shown).

The Filament: At Point Sur, the offshore flow associated with the filament of cold, chlorophyll-rich, upwelled water was observed early on cruise day 4 on the inshore end of the southern transect (*F*, stations 37–41, Figs. 9C, D). The filament was sampled during its initial growth. A thin layer was found at station 38, while station 37 displayed a broader subsurface fluorescence maximum on the same isopycnal (Fig. 14C). The ADCP-measured currents at $z = 19\,\mathrm{m}$ indicated convergence north of the filament and a jet of westward current at the thin layer and adjacent subsurface chlorophyll maximum (stations 37–38, Fig. 9D). The thin layer was located in sheared flow (*F*, station 38, Fig. 14F) and in the stratified transition layer (Fig. 14I).

5. Discussion and summary

5.1. Thin layer characteristics

Thin layers of phytoplankton were observed during cruises 2 and 3 (21–25 August and 3–6 September 2003) in the coastal upwelling zone near Monterey Bay, California. Some thin layers may have extended at least 20 km. Peak fluorescence values were $7-30\,\mathrm{mg\,m^{-3}}$ and layers were 1–5 m thick in the vertical at full width half maximum. The thickness of the observed thin layers is in rough agreement with numerical simulations of thin layer formation by steady shear, which yield a thickness on the order of 1 m (Birch et al., 2008). Bottle chlorophyll samples show fluorometer chlorophyll readings may have been 1.3−1.5× too large, but the scatter in this relation was considerable especially at the larger fluorescence values detected in thin layers. This affects neither layer thicknesses nor conclusions made in this paper. Cruises 2 and 3 took place during relaxations from upwelling conditions which began 3–4 days before each cruise.

Please cite this article as: Johnston, T.M.S., et al., Thin phytoplankton layer formation at eddies, filaments, and fronts in a coastal upwelling zone. Deep-Sea Research II (2008), doi:10.1016/j.dsr2.2008.08.006

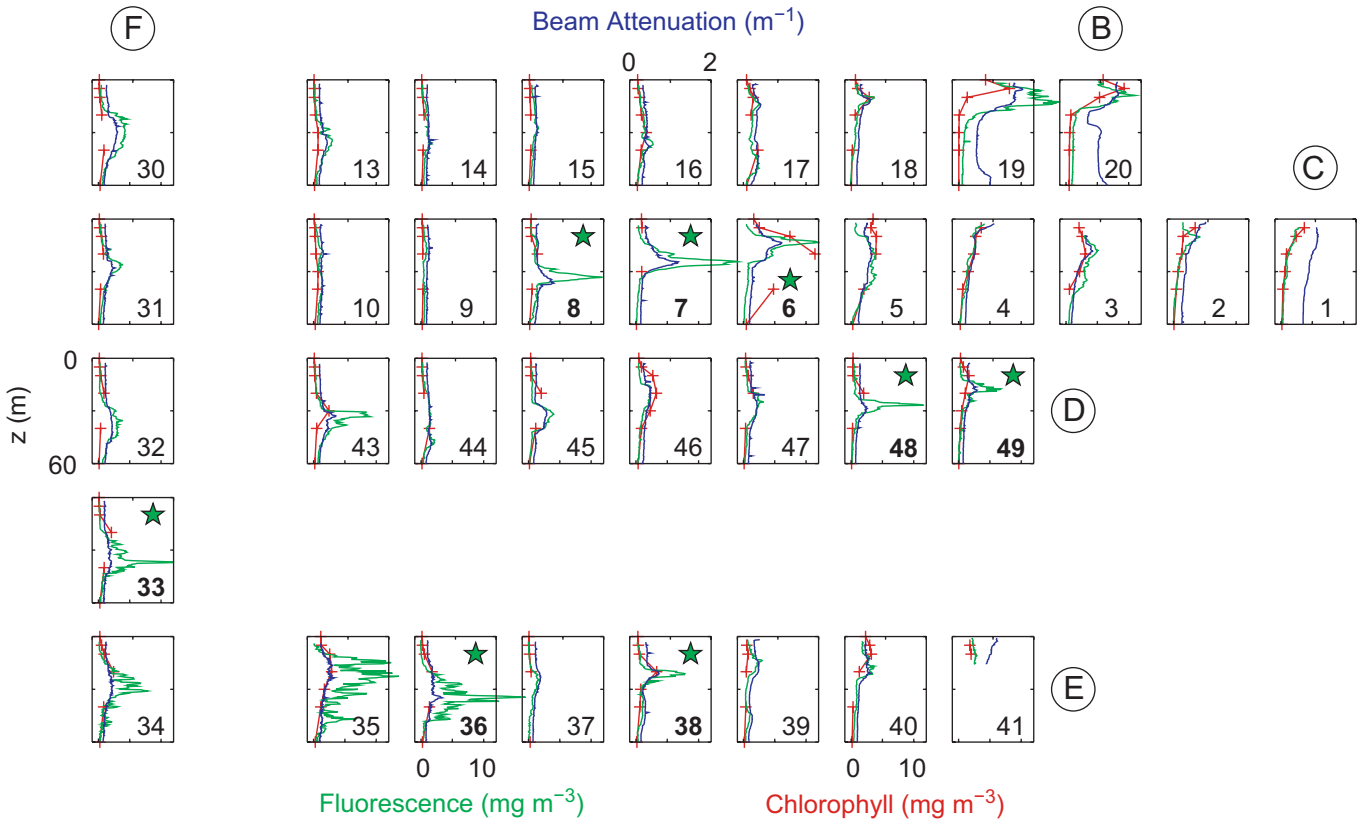

Fig. 11. As for Fig. 5, but for transects B–F on cruise 3.

Table 2
Subsurface fluorescence peaks at the upwelling tongue, filament, and eddies for cruise 3

Stn.	z_{max} (m)	F_{max} (mg m^{-3})	z_{fwhm} (m)	σ_θ (kg m^{-3})	Thin layer
6	13.4	12.1	4.8	25.05	Yes
7	24.4	16.3	3.9	25.02	Yes
8	33.4	11.8	4.2	25.06	Yes
33	36.9	14.0	0.9	24.68	Yes
34	31.0	7.9	11.3	24.58	
35	22.6	13.6	34.8	24.74	
36	34.5	16.7	3.3	24.75	Yes
37	24.7	1.7	12.8	24.59	
38	21.1	7.8	3.6	24.59	Yes
43	33.4	9.1	8.0	24.42	
48	26.8	11.5	1.5	24.62	Yes
49	17.6	6.8	4.5	24.48	Yes

Entries as in Table 1.

Assuming the thin layers began forming during the onset of relaxation (Churnside, 2007), our inferred persistence of 3–4 days is in rough agreement with a model estimate of 1.5 days (Birch et al., 2008).

On cruises 2 and 3, recently upwelled water was present at the Points Año Nuevo and Sur upwelling centers. The phytoplankton were entrained by eddies, fronts, and filaments. Thin layers were found at sheared flow on the flanks of these eddies, fronts, and filaments. These thin layers were located within the transition layer, a region of maximum shear and stratification at the base of the mixed layer. Elsewhere fluorescence was found as a broad subsurface maximum. Thin layers were not present in water of offshore origin.

5.2. Absence of thin layers on cruise 1

No thin layers were found on cruise 1 (2–6 August 2003) perhaps because weak winds were seen for 13 days prior to and during the entire cruise (Fig. 2). Weak upwelling was indicated by surface temperatures that were warmer and chlorophyll values that were only elevated within a few kilometers of the coast and that were an order of magnitude lower than on subsequent cruises. Mesoscale current shear from the thermal wind equation was an order of magnitude lower than on subsequent cruises. If thin layers are formed during relaxation events by mesoscale shear acting on recently upwelled phytoplankton-rich water, the 13-day relaxation is an order of magnitude longer time than the expected persistence of thin layers from the Birch et al. (2008) model. Based on our experiences during cruises 2 and 3 and the statistics of Churnside (2007) showing thin layers over 19% of their surveyed area during relaxations, we would likely have found thin layers had they been present at 4–9 stations out of the total 49.

Towed-body measurements with much better spatial coverage and vertical and horizontal resolution also revealed no thin layers, when upwelling resumed between cruises 1 and 2. Fluorescence measurements from the towed body showed subsurface maxima at the mouth of Monterey Bay (J. Ryan, personal communications), but thin layers were not found consistent with other observations during upwelling conditions (Churnside, 2007).

5.3. Shear and stratification

Current shear and stratification supported the formation of thin layers during the relaxation conditions on cruises 2 and 3. Shear stretched broad chlorophyll maxima of limited lateral

Please cite this article as: Johnston, T.M.S., et al., Thin phytoplankton layer formation at eddies, filaments, and fronts in a coastal upwelling zone. Deep-Sea Research II (2008), doi:10.1016/j.dsr2.2008.08.006

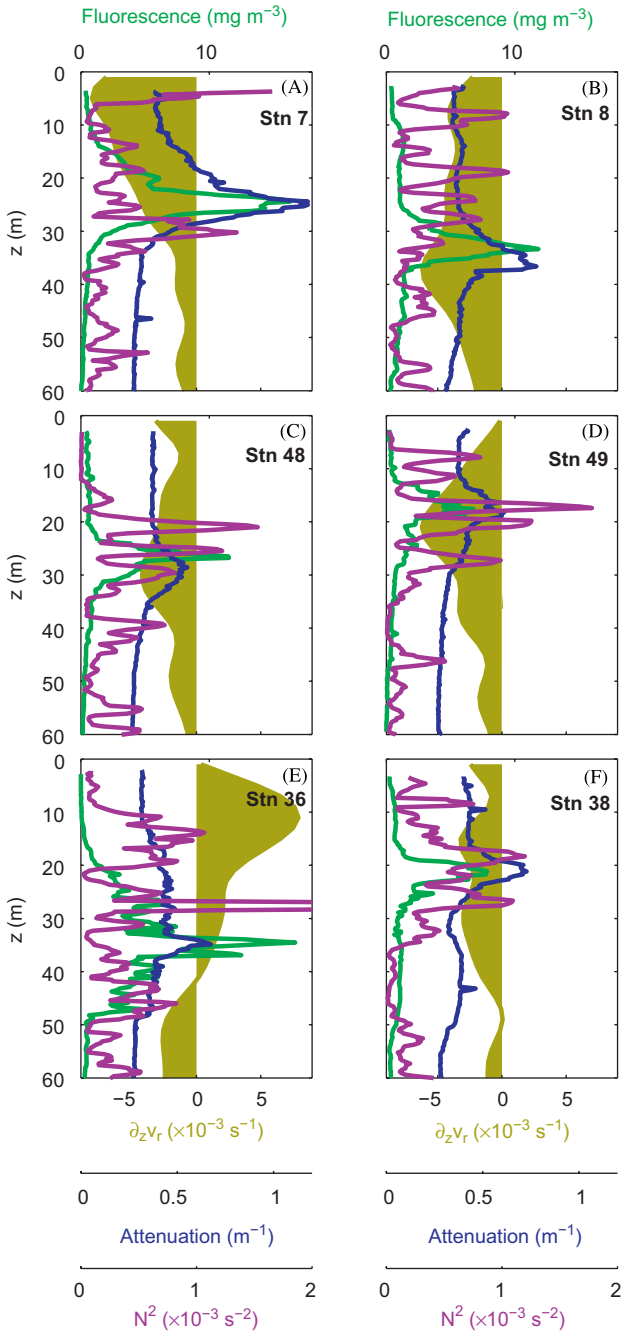

Fig. 12. Individual profiles of some stations with thin layers similar to Fig. 6, but for cruise 3. Thin layers are found at: (A) station 7, (B) station 8, (C) station 48, (D) station 49, (E) station 36, and (F) station 38. Note the scales are different from Fig. 6.

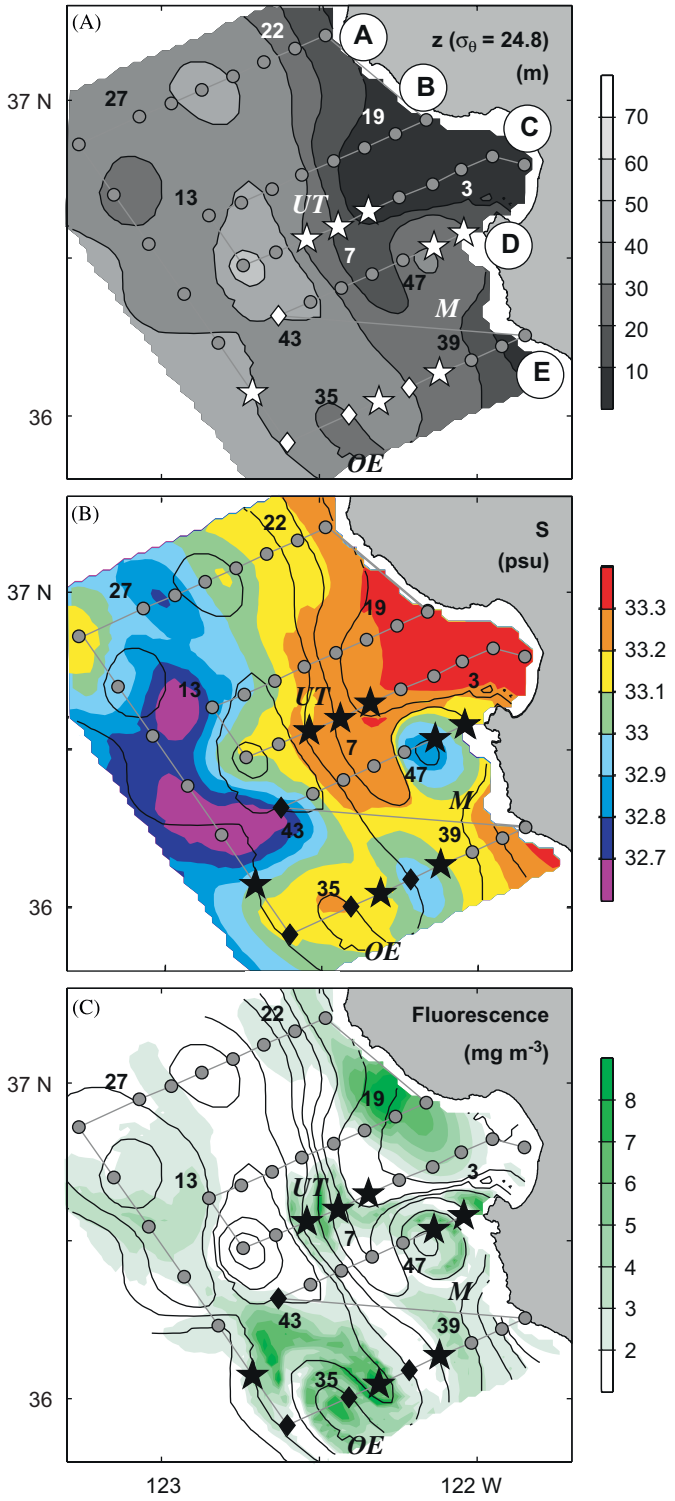

Fig. 13. (A) Depths of the $\sigma_\theta = 24.8\,\mathrm{kg\,m^{-3}}$ isopycnal for cruise 3 are plotted and contoured (black) in 10- and 5-m intervals in (B) and (C). (B) Salinity and (C) fluorescence are plotted on $\sigma_\theta = 24.8\,\mathrm{kg\,m^{-3}}$. Gray dots indicate CTD stations, stars indicate thin layer locations, and diamonds indicate nearby subsurface chlorophyll maxima. The upwelling tongue (*UT*), meander (*M*), and offshore eddy (*OE*) are labeled (Section 4.3).

extent at the coast (~40 km alongshore, 20 km cross-shore, and 30 m thick) into elongated and vertically thin layers. This shearing also increased vertical gradients. The stratified transition layer inhibited the penetration of wind-driven vertical mixing enabling these thin layers to persist in the environment. The light winds on cruises 2 and 3 further reduced vertical mixing.

Geostrophic current shear in this paper was calculated from horizontal density gradients via the thermal wind equation and therefore underestimated shear for a variety of reasons. Ageostrophic processes (e.g., near-inertial motions, internal waves, and accelerating flow at developing filaments) contributed to the total shear. Shear of cross-shore currents at filaments, for example, was also either not detected or underestimated by our method. At fronts and in the transition layer, shear is mostly not in geostrophic balance due to near-inertial motions and thus our calculations underestimated shear (Rudnick and Luyten, 1996; Plueddemann and Farrar, 2006).

Please cite this article as: Johnston, T.M.S., et al., Thin phytoplankton layer formation at eddies, filaments, and fronts in a coastal upwelling zone. Deep-Sea Research II (2008), doi:10.1016/j.dsr2.2008.08.006

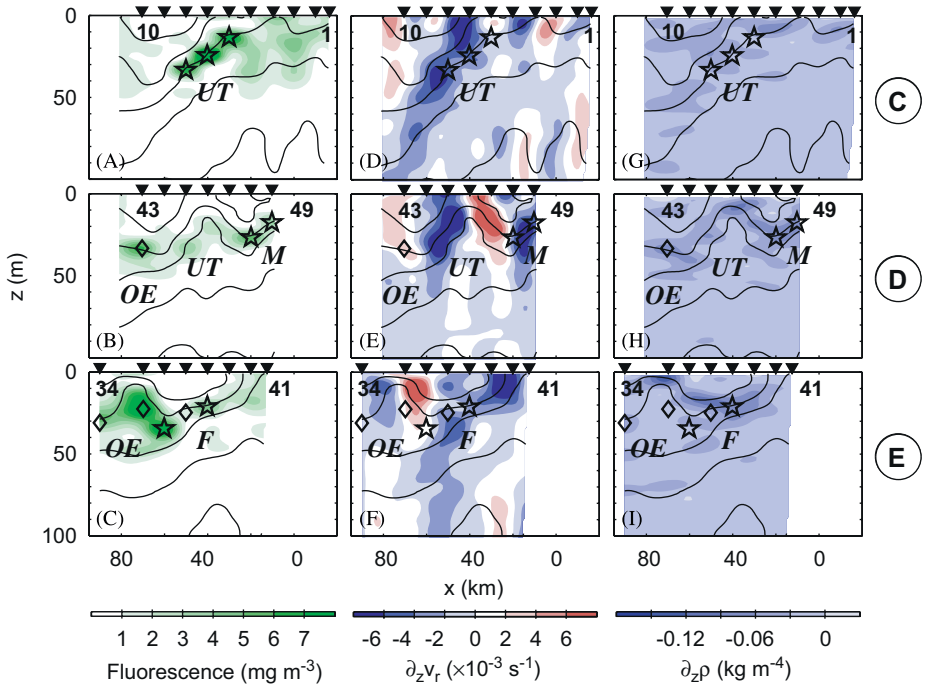

Fig. 14. For cruise 3, cross-shore transects C–E (from north to south; top to bottom of page) of fluorescence (left column, A–C), alongshore geostrophic current shear from the thermal wind equation (middle column, D–F), and vertical density gradient (right column, G–I). x is the cross-shore distance from station 3 on transect C. Contours are $\sigma_\theta = 24.0$, 24.5, 25.0, 25.5, and 26.0 kg m^{-3}. Black triangles indicate CTD stations. Station numbers are noted at the east and west ends of the transects. The upwelling tongue (*UT*), meander (*M*), filament (*F*), and offshore eddy (*OE*) are labeled (Section 4.3). Thin layers are indicated with stars and nearby subsurface chlorophyll maxima are denoted with diamonds.

5.4. Extent of thin layers

During cruise 3, we found thin layers at the *UT* on the same isopycnal at three adjacent stations (with 10-km station separation) over a distance of 20 km, which suggests the thin layer was continuous over this distance. However, a finer-resolution survey with additional bio-optical measurements and species composition data would be needed for confirmation. Continuous thin layers extending from 1 to 10 km have been observed by optical instruments mounted on aircraft (Churnside, 2007).

At the *AE* or meander on cruise 3, thin layers at two adjacent stations were separated by 10 km. These layers were not on the same isopycnal. Shear acting on a fluorescence patch of limited vertical extent will produce a continuous thin layer at different density levels (Birch et al., 2008). This scenario seems especially likely at a coastal upwelling center.

On cruise 2, thin layers were found at the base and the offshore tip of a 100-km long filament, while broader subsurface chlorophyll maxima were found along the filament. These layers were not continuous, but this result suggests that higher-resolution sampling along a filament may find thin layers forming and dissipating along much of its length and possibly extending tens of kilometers.

5.5. High chlorophyll concentrations in thin layers

Higher chlorophyll concentrations were often found in thin layers than in the subsurface chlorophyll maxima at the upwelling centers. This result is unexplained by our data. We speculate below on possible mechanisms for the increased concentrations. Shear and stratification do explain the thinning of subsurface chlorophyll maxima into thin layers and their persistence. However, shear cannot produce higher concentrations. Conditions were possibly conducive to *in situ* growth. The same shearing and stirring processes, which increase gradients of phytoplankton, can increase gradients and thus fluxes of other quantities, such as nutrients. The phytoplankton may have benefited from their location in the transition layer, a region of intermediate turbulence compared to the mixed layer or the weakly stratified oceanic interior. There are other possible explanations. Convergent vertical fluxes due to a decrease in sinking at density gradients could increase phytoplankton concentrations (Derenbach et al., 1979; MacIntyre et al., 1995), but based on the one-dimensional model of Hodges and Rudnick (2004) this convergence will not form thin layers (B. Hodges, personal communications). Turbulent mixing in the transition layer can resuspend sinking phytoplankton aggregations (MacIntyre et al., 1995). Also chlorophyll content within cells can change in response to light and nutrient history (Eisner and Cowles, 2005; Sutor et al., 2005).

5.6. Summary

Previous work and our results indicate that thin layers are commonly found (1) in coastal upwelling zones where recently upwelled water encounters sheared flow on the flanks of eddies, fronts, and filaments and (2) in the transition layer where stratification and shear are the strongest and high vertical gradients are found in other properties (McManus et al., 2005; Ryan et al., 2005; Sutor et al., 2005; Churnside, 2007). A simple advection–diffusion model of current shear acting on tracer patches of limited extent show that thin layers should be ubiquitous (Birch et al., 2008). The strongly stratified transition layer also inhibits penetration of weak wind-driven vertical mixing during relaxations. These results raise the question: Are the high phytoplankton concentrations due to successful exploitation of an ecological niche or simply a consequence of the physics? Further progress requires three-dimensional surveys with wide spatial coverage and fine spatial and temporal

Please cite this article as: Johnston, T.M.S., et al., Thin phytoplankton layer formation at eddies, filaments, and fronts in a coastal upwelling zone. Deep-Sea Research II (2008), doi:10.1016/j.dsr2.2008.08.006

resolution of bio-optical data, current shear, stratification, and turbulent mixing in the transition layer during relaxations and upwellings at mesoscale features, such as eddies, filaments, and fronts.

Acknowledgments

We thank the scientists and crew aboard the R/V *Point Sur* for their assistance gathering the data. Coastal surface current data from CODAR were provided by Jeff Paduan (Naval Postgraduate School) and Bruce Lipphardt (University of Delaware). AVHRR data are courtesy of NOAA NWS Monterey Regional Office and NOAA CoastWatch. SeaWiFS data are courtesy of the Monterey Bay Aquarium Research Institute; University of California, Santa Cruz; Orbimage Inc.; and NOAA CoastWatch. This work was funded by the Office of Naval Research's Grant N000140310267 to Margaret McManus and Francisco Chavez. Support was also provided by the David and Lucile Packard Foundation. Comments from John Ryan (Monterey Bay Aquarium Research Institute) and two anonymous reviewers greatly improved the manuscript.

References

Birch, D.A., Young, W.R., Franks, P.J.S., 2008. Thin layers of phytoplankton: formation by shear and death by diffusion. Deep-Sea Research I 55, 277–295.

Capet, X., McWilliams, J.C., Molemaker, M.J., Shchepetkin, A.F., 2008. Mesoscale to submesoscale transition in the California Current System. Part I: flow structure, eddy flux, and observational tests. Journal of Physical Oceanography 38, 29–43.

Churnside, J.H., 2007. LIDAR detection of plankton in the ocean. In: International Geoscience and Remote Sensing Symposium, Barcelona, Spain.

Collins, C.A., Pennington, J.T., Castro, C.G., Rago, T.A., Chavez, F.P., 2003. The California Current System off Monterey, California: physical and biological coupling. Deep-Sea Research II 50, 2389–2404.

Cowles, T.J., Desiderio, R.A., Neuer, S., 1993. In situ characterization of phytoplankton from vertical profiles of fluorescence emission spectra. Marine Biology 115, 217–222.

Davis, R.E., Leonard, N.E., Fratantoni, D.M., 2008. Routing strategies for underwater gliders. Deep-Sea Research II, this issue [doi:10.1016/j.dsr2.2008.08.005].

Dekshenieks, M.M., Donaghay, P.L., Sullivan, J.M., Rines, J.E.B., Osborn, T.R., Twardowski, M.S., 2001. Temporal and spatial occurrence of thin phytoplankton layers in relation to physical processes. Marine Ecology Progress Series 223, 61–71.

Derenbach, J.B., Astheimer, H., Hansen, H.P., Leach, H., 1979. Vertical microscale distribution of phytoplankton in relation to the thermocline. Marine Ecology Progress Series 1, 187–193.

Dever, E.P., 2004. Objective maps of near-surface flow states near Point Conception, California. Journal of Physical Oceanography 34, 444–461.

Donaghay, P.L., Osborn, T.R., 1997. Toward a theory of biological–physical control of harmful algal bloom dynamics and impacts. Limnology and Oceanography 42, 1283–1296.

Donaghay, P.L., Rimes, H.M., Sieburth, J.McN., 1992. Simultaneous sampling of fine scale biological, chemical and physical structure in stratified waters. Archiv für Hydrobiologie Beiheft Ergebnisse Limnologie 36, 97–108.

Eisner, L.B., Cowles, T.J., 2005. Spatial variations in phytoplankton pigment ratios, optical properties, and environmental gradients in Oregon coast surface waters. Journal of Geophysical Research 110, C10S14, doi:10.1029/2004JC002614.

Franks, P.J.S., 1995. Thin layers of phytoplankton: a model of formation by near-inertial wave shear. Deep-Sea Research I 42, 75–91.

Franks, P.J.S., Jaffe, J.S., 2001. Microscale distributions of phytoplankton: initial results from a two-dimensional imaging fluorometer. OSST Marine Ecology Progress Series 220, 59–72.

Gill, A.E., 1982. Atmosphere-Ocean Dynamics. Academic Press, San Diego, p. 662.

Hodges, B.A., Rudnick, D.L., 2004. Simple models of steady deep maxima in chlorophyll and biomass. Deep-Sea Research I 51, 999–1015.

Holliday, D.V., Donaghay, P.L., Greenlaw, C.F., McGehee, D.E., McManus, M.A., Sullivan, J.M., Miksis, J.L., 2003. Advances in defining fine- and micro-scale pattern in marine plankton. Aquatic and Living Resources 16, 131–136.

Jachec, S.M., Fringer, O.B., Gerritsen, M.G., Street, R.L., 2006. Numerical simulation of internal tides and the resulting energetics within Monterey Bay and the surrounding area. Geophysical Research Letters 33, L12605, doi:10.1029/2006GL026314.

Johnston, T.M.S., Rudnick, D.L., 2008. Observations of the transition layer. Journal of Physical Oceanography, in press, doi:10.1175/2008JPO3824.1.

Kunze, E., Rosenfeld, L.K., Carter, G.S., Gregg, M.C., 2002. Internal waves in Monterey Submarine Canyon. Journal of Physical Oceanography 32, 1890–1913.

Lavender, K.L., 2001. The general circulation and open-ocean deep convection in the Labrador Sea: a study using subsurface floats. Ph.D. Dissertation, University of California, San Diego, 131pp.

Le Traon, P.-Y., 1990. A method for optimal analysis of fields with spatially-variable mean. Journal of Geophysical Research 95, 13543–13547.

Lunven, M., Guillaud, J.F., Youénou, A., Crassous, M.P., Berric, R., Le Gall, E., Kérouel, R., Labry, C., Aminot, A., 2005. Nutrient and phytoplankton distribution in the Loire River pllume (Bay of Biscay, France) resolved by a new Fine Scale Sampler. Estuarine, Coastal, and Shelf Science 65, 94–108.

Maar, M., Nielsen, T.G., Stips, A., Visser, A.W., 2003. Microscale distribution of zooplankton in relation to turbulent diffusion. Limnology and Oceanography 48, 1312–1325.

MacIntyre, S., Alldredge, A.L., Gotschalk, C.C., 1995. Accumulation of marine snow at density discontinuities in the water column. Limnology and Oceanography 40, 449–468.

Mahadevan, A., Campbell, J.W., 2002. Biogeochemical patchiness at the sea surface. Geophysical Research Letters 29, 1926, doi:10.1029/2001GL014116.

McManus, M.A., Alldredge, A.L., Barnard, A., Boss, E., Case, J., Cowles, T.J., Donaghay, P.L., Eisner, L., Gifford, D.J., Greenlaw, C.F., Herren, C., Holliday, D.V., Johnson, D., MacIntyre, S., McGehee, D., Osborn, T.R., Perry, M.J., Pieper, R., Rines, J.E.B., Smith, D.C., Sullivan, J.M., Talbot, M.K., Twardowski, M.S., Weidemann, A., Zaneveld, J.R.V., 2003. Characteristics, distribution and persistence of thin layers over a 48 h period. Marine Ecology Progress Series 261, 1–19.

McManus, M.A., Cheriton, O.M., Drake, P.J., Holliday, D.V., Storlazzi, C.D., Donaghay, P.L., Greenlaw, C.F., 2005. Effects of physical processes on structure and transport of thin zooplankton layers in the coastal ocean. Marine Ecology Progress Series 310, 199–215.

Osborn, T.R., 1998. Finestructure, microstructure, and thin layers. Oceanography 11, 36–43.

Paduan, J., Lipphardt, B., 2003. Coastal Ocean Dynamics Applications Radar (CODAR) Data, August 2003. Autonomous Ocean Sampling Network (AOSN) 2003 Field Experiment. Retrieved from ⟨http://aosn.mbari.org⟩.

Pennington, J.T., Chavez, F.P., 2000. Seasonal fluctuations of temperature, salinity, nitrate, chlorophyll and primary production at station H3/M1 over 1989–1996 in Monterey Bay, California. Deep-Sea Research II 47, 947–973.

Petruncio, E.T., Rosenfeld, L.K., Paduan, J.D., 1998. Observations of the internal tide in Monterey Canyon. Journal of Physical Oceanography 28, 1873–1903.

Plueddemann, A.J., Farrar, J.T., 2006. Observations and models of the energy flux to mixed-layer inertial currents. Deep-Sea Research II 53, 5–30.

Ramp, S.R., Paduan, J.D., Shulman, I., Kindle, J., Bahr, F.L., Chavez, F., 2005. Observations of upwelling and relaxation events in the northern Monterey Bay during August 2000. Journal of Geophysical Research 110, C07013.

Ramp, S.R., Davis, R.E., Leonard, N.E. Shulman, I., Chao, Y., Robinson, A.R., Mardsen, J., Lermuisiaux, P., Fratantoni, D., Paduan, J.D., Chavez, F., Bahr, F.L., Liang, S., Leslie, W., Li, Z., 2008. Preparing to predict: the second autonomous ocean sampling network (AOSN-II) experiment in the Monterey Bay. Deep-Sea Research II, this issue [doi:10.1016/j.dsr2.2008.08.013].

Rines, J.E.B., Donaghay, P.L., Dekshenieks, M.M., Sullivan, J.M., Twardowski, M.S., 2002. Thin layers and camouflage: hidden pseudo-nitzschia populations in a fjord in the San Juan Islands, Washington, USA. Marine Ecology Progress Series 225, 123–137.

Rosenfeld, L.K., Schwing, F.B., Garfield, N., Tracy, D.E., 1994. Bifurcated flow from an upwelling center: a cold water source for Monterey Bay. Continental Shelf Research 14, 931–964.

Roughan, M., Mace, A.J., Largier, J.L., Morgan, S.G., Fisher, J.L., Carter, M.L., 2005. Subsurface recirculation and larval retention in the lee of a small headland: a variation on the upwelling shadow theme. Journal of Geophysical Research 110, C10027.

Rudnick, D.L., Luyten, J.R., 1996. Intensive surveys of the Azores Front, 1. Tracers and dynamics. Journal of Geophysical Research 101, 923–939.

Ryan, J.P., Chavez, F.P., Bellingham, J.G., 2005. Physical–biological coupling in Monterey Bay, California: topographic influences on phytoplankton ecology. Marine Ecology Progress Series 287, 23–32.

Strub, P.T., Kosro, P.M., Huyer, A., CTZ Collaborators, 1991. The nature of cold filaments in the California Current System. Journal of Geophysical Research 96, 14743–14768.

Sutor, M.M., Cowles, T.J., Peterson, W.T., Pierce, S.D., 2005. Acoustic observations of finescale zooplankton distributions in the Oregon upwelling region. Deep-Sea Research II 52, 109–121.

Thomas, L., 2008. Formation of intrathermocline eddies at ocean fronts by wind-driven destruction of potential vorticity. Dynamics of Atmospheres and Oceans 45, 252–273.

Wang, X., Chao, Y., Dong, C., Farrara, J., Li, Z., McWilliams, J.C., Paduan, J.D., Rosenfeld, L.K., 2008. Modeling tides in Monterey Bay, California. Deep-Sea Research II, this issue [doi:10.1016/j.dsr2.2008.08.012].

Wolk, F., Yamazaki, H., Seuront, L., Lueck, R.G., 2002. A new free-fall profiler for measuring biophysical microstructure. Journal of Atmospheric and Oceanic Technology 19, 780–793.

Please cite this article as: Johnston, T.M.S., et al., Thin phytoplankton layer formation at eddies, filaments, and fronts in a coastal upwelling zone. Deep-Sea Research II (2008), doi:10.1016/j.dsr2.2008.08.006